JOURNAL OF GEOPHYSICAL RESEARCH, VOL. 104, NO. B4, PAGES 7089–7101, APRIL 10, 1999

A steady state conductive geotherm for the north central Slave, Canada: Inversion of petrological data from the Jericho Kimberlite pipe

James K. Russell and Maya G. Kopylova
Igneous Petrology Laboratory, Geological Sciences Division, Earth and Ocean Sciences
University of British Columbia, Vancouver, British Columbia, Canada

Abstract. Mantle xenoliths carried by kimberlite provide direct evidence for the rock types that constitute the roots to ancient cratons and provide critical constraints on the thermal state of the lithosphere. We derive a steady state conductive geotherm for the north central Slave craton based on published data for xenoliths from the Middle Jurassic Jericho kimberlite. The preferred model geotherm assumes a two-layer lithosphere. The upper layer is **D** km thick, has constant thermal conductivity, and an exponential decrease in heat production with depth ($\mathbf{Ao}\ e^{-z/D}$); **Ao** is a fixed value based on the bedrock geology. Below **D**, the lithosphere has a higher, constant thermal conductivity and a constant value of radiogenic heat production (**Am**). Inverting the thermobarometric data produces model estimates of surface heat flow ($\mathbf{q_o}$) and the depth-scale parameter (**D**) of 54.1 mWm^{-2}, and 25.8 km, respectively. The value of **D** corresponds to the thickness of upper to middle crust as defined by seismology for the southern Slave craton. On the basis of our analysis the Slave craton is characterized by high surface heat flow, relative to other Archean cratons, which is consistent with a single field measurement from the southern Slave craton. The high surface heat flow results from the high concentrations of radiogenic heat producing elements found in Slave crustal rocks. Despite the relatively high surface flow, the underlying lithosphere is cool relative to mantle beneath the rest of North America and other Archean cratons. The model geotherm predicts a thermal gradient in the mantle (100-200 km) of between 5.0 and 3.7 (°C/km) and a mantle heat flow of 15.9-11.9 mWm^{-2} that is consistent with other estimates of mantle heat flow beneath Precambrian continental crust.

1. Introduction

Over the past decade, geophysical [*Clowes*, 1997; *Cook et al.*, 1997; *Bostock and Cassidy*, 1997] and petrological [*Kjarsgaard*, 1996; *Pell*, 1997; *Boyd and Canil*, 1997; *Kopylova et al.*, 1998a; b; *Pearson et al.*, 1998] investigations of the Slave Province, Northwest Territories, Canada, have elucidated the nature of the deep mantle underlying this Archean craton [e.g., *Padgham and Fyson*, 1992; *Percival*, 1996]. The presence of diamondiferous kimberlite across the Northwest Territories (Figure 1) has served as a catalyst for petrological research by providing access to deep-seated, mantle-derived xenoliths [e.g., *Kjarsgaard and Petersen*, 1992; *Kopylova et al.* 1998a]. Following more or less established methodologies [e.g., *Finnerty and Boyd*, 1987; *O'Reilly and Griffin*, 1996], these suites of xenoliths have been used to define the composition, thermal state [e.g., *Kopylova et al.*, 1998a; *Boyd and Canil*, 1997; *MacKenzie and Canil*, 1997], structure, and stratigraphy [*Kopylova et al.*, 1998a; c] of the upper mantle underlying the Slave craton. The thermal structure of the Slave lithosphere, in particular, has garnered attention [e.g., *Grotzinger and Royden*, 1990] because of the implications for the exploration of diamondiferous kimberlite [*Thompson et al.*, 1995b, 1996; *Kopylova et al.*, 1998b].

Below we derive a paleo-geotherm for the north central Slave craton using thermobarometric data for 37 mantle-derived xenoliths (Table 1) from the Jericho pipe [*Kopylova et al.*, 1998b]. The Jericho pipe is located 400 km NE of Yellowknife near the northern end of Contwoyto Lake (Figure 1), is dated at 172 ±3 Ma [*Heaman et al.*, 1998] and contains significant diamond. Our approach is to fit an analytical expression for a composite, two-layer, one-dimensional model for steady state conductive heat transfer to the pressure-temperature (P-T) data array. The result is that we indirectly constrain some of the heat flow parameters for the paleo-lithosphere underlying this portion of the Slave craton. The model developed here represents a refinement on a previous model for the geotherm used by *Kopylova et al.* [1998b], which did not differentiate, in terms of thermal properties, between crust and mantle within the lithospheric column.

Paper number 1999JB900012.
0148-0227/99/ 1999JB900012$09.00

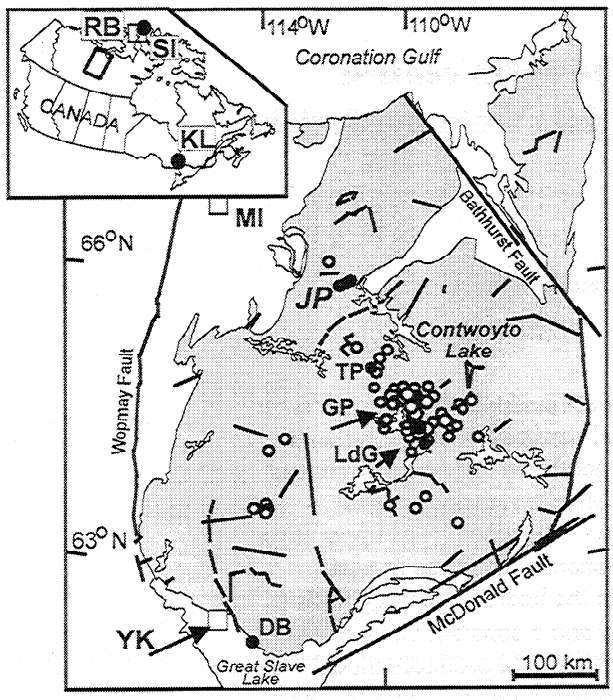

Figure 1. Tectonic map of Slave craton, Northwest Territories, Canada (see inset) showing locations of Jericho (JP), Grizzly (GP), Torrie (TP), Drybones (DB) and Lac de Gras (LdG) kimberlite pipes against distribution of other kimberlite bodies within craton (modified after *Padgham and Fyson* [1992] and *Kjarsgaard* [1996]). Also shown are locations of Somerset Island (SI) and Kirkland lake (KL) kimberlites and heat flow measurement locations near Yellowknife (YK [*Lewis and Wang*, 1992]), Muskox intrusion (MI [*Beck and Sass*, 1966]) and Resolute Bay (Inset, RB [*Lachenbruch*, 1957].

This "inversion" of P-T data for model heat flow parameters offers an alternative to other approaches. A more common approach is to match thermobarometric data against standardized steady state conductive geotherms that use average models for continental or oceanic lithosphere [e.g., *Pollack and Chapman*, 1977; *Chapman*, 1986]. As discussed by *Rudnick et al.* [1998], the interpretation of such geotherms can be problematical where the lithosphere does not have average properties. A second approach involves forward modeling of geotherms for a specific and assumed crust-mantle configuration [*Cull et al.*, 1991; *Bussod and Williams*, 1991; *Thompson et al.*, 1996]. The resulting geotherms can be highly sensitive to the architecture and composition of the crust and mantle [e.g., *Chapman*, 1986; *Rudnick* et al., 1998] and can produce misleading results if the assumed configuration is in error.

Our approach is relatively independent of assumptions about crustal structure and therefore is especially well-suited to regions with sparse geophysical data or for deducing ancient geotherms. The main geological parameter used for the "inverse modeling" is surface heat generation, which derives from a knowledge of local geology and geochemistry. We conclude with a geotherm that best fits the data of *Kopylova et al.* [1998b] and that constrains the lithospheric architecture of the Slave craton at the time of emplacement for the Jericho kimberlite pipe.

2. Xenolith Thermobarometry

Kimberlite magmas sample the Earth at depths exceeding 200 km and transport samples of mantle at time scales less than the time scales of most magmatic reactions [*Edwards and Russell*, 1996]. As advocated by *O'Reilly and Griffin* [1996], these exotic materials provide unparalleled opportunities for mapping the subcontinental lithosphere. Central to this exercise is the ability to assign equilibrium P-T conditions to each xenolith.

On the basis of observations and data of *Kopylova et al.* [1998b] we present P-T points for each peridotite and pyroxenite xenolith (Table 1), derived from compositions of coexisting garnet-clinopyroxene-orthopyroxene, using (1) the methods of *Brey and Kohler* [1990] (hereinafter referred to as BK) and (2) the geothermometer of *Finnerty and Boyd* [1987], in conjunction with the geobarometer of *MacGregor* [1974] (hereinafter referred to as FB-MG). The two calculational schemes produce systematic differences in estimated mantle temperatures and pressures of $\Delta T \approx 60°C$ and $\Delta P \approx 2$ kb (Figures 2 and b). However, the geometries of the P-T arrays are parallel (Figure 2c) and predict a similar thermal structure. We have used mainly the results from the *Brey and Kohler* [1990] model (Figure 2d). Figure 2d shows calculated P-T conditions for two populations of peridotitic and pyroxenitic xenoliths from the mantle: (1) material which is interpreted to have equilibrated with a steady state conductive geotherm and (2) material derived from a disturbed portion of the geotherm [*Kopylova et al.*, 1998a, b]. Only samples that appear to have equilibrated with the undisturbed portion of the geotherm (see Table 3) are used for modeling.

3. A Model Geotherm

3.1. The Model Equation

Below we develop a one-dimensional, steady state conductive geotherm model [e.g., *Lachenbruch*, 1968; *Crowley*, 1987; *Fowler*, 1990; *Cermak et al.*, 1991] that describes the temperature distribution in the lithosphere beneath the Slave Craton. We adopt a composite, two-layer model [e.g., *Fowler*, 1990] in which the individual layers have unique values of thermal conductivity (**K**) and unique distributions of heat producing elements (HPE). We then fit the derived analytical expression to our thermobarometric data.

Figure 3 is a schematic representation of the heat flow model. The upper layer (layer 1), of thickness **D** (km), has constant surface temperature ($\mathbf{T_s}$), thermal conductivity ($\mathbf{K_1}$), and surface heat flow ($\mathbf{q_o}$). Initially, we assume that radiogenic heat sources within layer 1 decrease exponentially with depth (Figure 3b):

$$A_1(z) = Ao\, e^{-z/D} \qquad (1)$$

where **Ao** represents the mean heat generation capacity of surface crustal rocks (Figure 3b). We also consider, for comparative purposes, an upper layer with a uniform

Table 1. P-T Determinations on Xenoliths From Jericho Kimberlite Pipe

Rock Type	Texture	Sample	T[a],°C	P[b],Kbar	T[c],°C	P[c],Kbar
Spinel plus Garnet	coarse	4-2	888	45.3	932	49.4
Peridotite		25-4	868	41.2	975	47.7
		21-1	786	31.3	811	30.8
		9-2	705	28.8	809	32.8
		22-5	892	42.6	951	42.9
		41-4	560	19.3	648	25.2
		22-1	520	14.4	690	26.7
		22-4	747	32.7	833	36
		40-7	886	42.2	967	44.8
		26-11	851	39.3	944	42.7
		26-3	766	34.3	833	35.9
Garnet Peridotite	coarse	14-77	855	40.5	912	41.6
		25-9	781	35.3	842	36.6
		4-3	825	38.4	921	42.2
		14-107	970	48.9	1068	51.6
		40-11	1048	55.2	1104	52.1
		21-6	1094	57	1190	62.2
		26-3	766	34.3	833	35.9
		5-3	817	37.6	918	41
		21-4	1019	51.7	1097	55.2
Garnet Peridotite	porphyroclastic	21-2	1287	65.2	1335	57.7
		22-7	1121	57.7	1187	53.4
		23-5	1193	58.5	1262	59.2
		40-9	1247	63	1297	56
		41-1	1217	60.5	1274	55.5
		40-21	1215	60.6	1273	54.7
		40-36	1184	60.2	1245	53.5
		8-1	1228	61.4	1282	56.4
		14-78	1236	62	1300	59
		21-3	994	48.7	1088	51.2
		40-38	1228	62.2	1286	49.5
		40-5	1251	63.5	1300	54.4
Garnet Pyroxenite	megacrystalline	26-12	1135	57.1	1246	65.1
		9-10	1126	56.6	1214	62.9
		14-124	1121	56.9	1230	64.2
		14-105	1115	56.5	1205	60
		41-3	1213	59.1	1281	60

[a] *Finnerty and Boyd* [1987].
[b] *MacGregor* [1974].
[c] *Brey and Kohler* [1990].

distribution (**Ao**) of HPE (Figure 3b). The underlying medium (layer 2) has uniform thermal conductivity ($\mathbf{K_2}$) and radiogenic heat production (**Am**). The temperature distribution for this composite, two-layer model derives from simultaneous solution of two boundary value problems. Temperature in the upper layer is described by solution of

$$\frac{\partial^2 T_1}{\partial^2 z} = \frac{-A_1(z)}{K_1} \qquad 0 < z < D \qquad (2a)$$

subject to boundary conditions

$$T_1 = T_s \qquad \text{for} \quad z = 0 \qquad (2b)$$

$$\frac{\partial T_1}{\partial z} = \frac{q_o}{K_1} \qquad \text{for} \quad z = 0 \qquad (2c)$$

The temperature distribution in layer 2 is given by solution of

$$\frac{\partial T_2}{\partial^2 z} = \frac{-A_2}{K_2} \qquad D < z < \infty \qquad (3a)$$

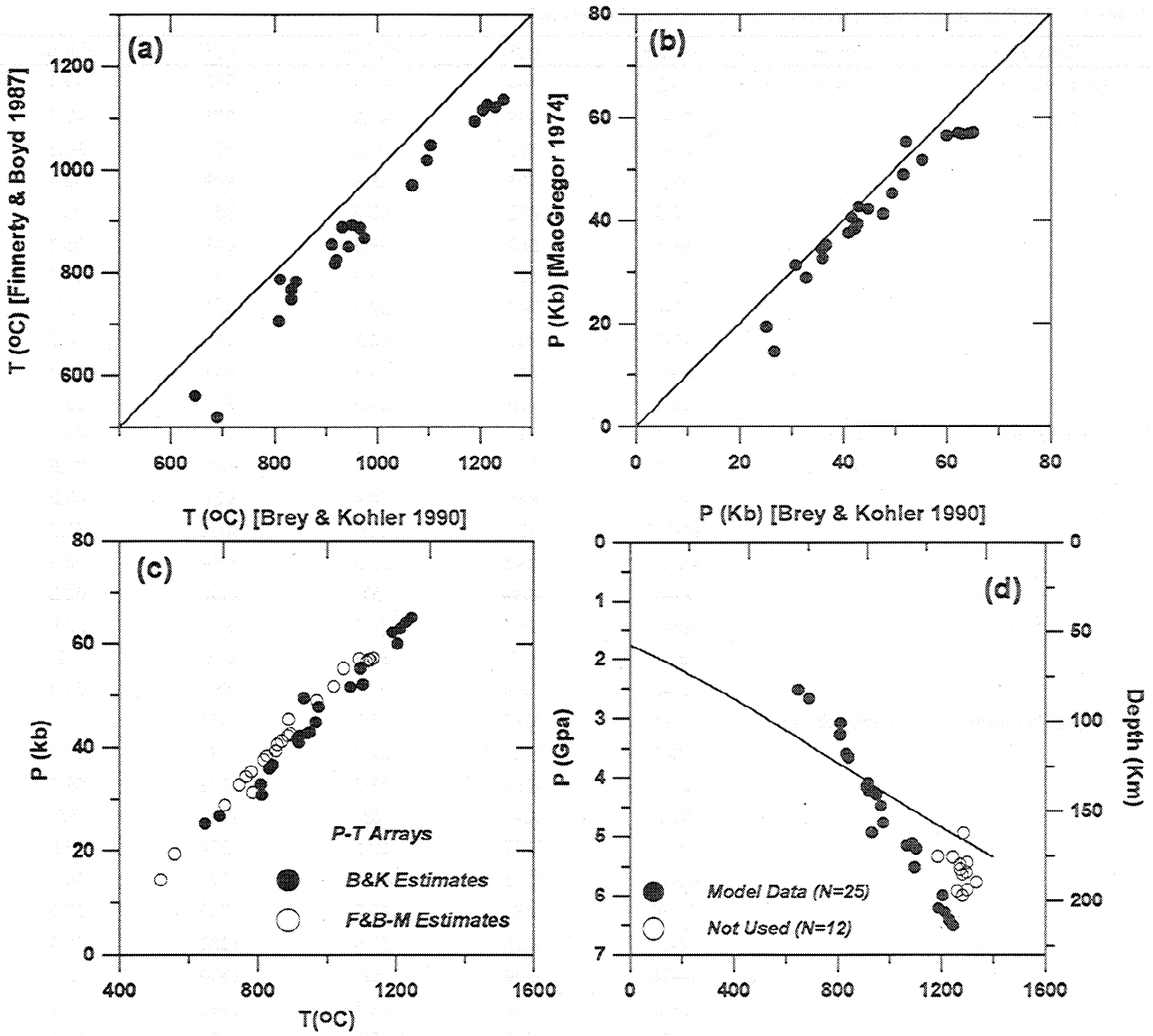

Figure 2. Thermobarometric results (Table 1) for mantle xenoliths recovered from the Jericho kimberlite, including P-T estimates derived from *Brey and Kohler* [1990] and from *Finnerty and Boyd* [1987] used in conjunction with *MacGregor* [1974]. Comparison is shown as estimates of (a) T(°C), (b) P(Kbar), and (c) P and T. (d) *Brey and Kohler* [1990] solution is shown for all peridotitic and pyroxenitic samples, relative to the diamond-graphite stability fields (solid line). Solid dots denote samples equilibrated with the geotherm and used for thermal modeling. Open symbols are samples from disturbed portion of the geotherm (see text).

subject to

$$T_2 = T_1 \qquad \text{for} \quad z = D \qquad (3b)$$

$$K_2 \frac{\partial T_2}{\partial z} = q_1 \qquad \text{for} \quad z = D \qquad (3c)$$

Solution of these boundary value problems yields two analytical expressions. Temperature in layer 1 is given by

$$T_1(z) = T_S + \frac{q_o z}{K_1} + \frac{A_o D^2}{K_1}\left[1 - \frac{z}{D} - e^{-z/D}\right] \qquad 0 < z < D. \qquad (4)$$

The temperature distribution in layer 2 is described by

$$T_2(z) = T_S + q_o\left[\frac{D}{K_1} - \frac{D-z}{K_2}\right] - \frac{A_m(D-z)^2}{2K_2} + A_o D\left[\frac{0.6321(D-z)}{K_2} - \frac{0.3679D}{K_1}\right] \qquad D < z < \infty. \qquad (5)$$

Figure 3 shows schematically the temperature distributions for both layers; as required by the boundary conditions the curves intersect exactly at a depth of **D**. Equation (5) shows explicitly how temperature in the deeper lithosphere ($z>D$) is coupled to parameters related to the crust, namely, q_o and **D**. Although surface heat flow and the **D** parameter

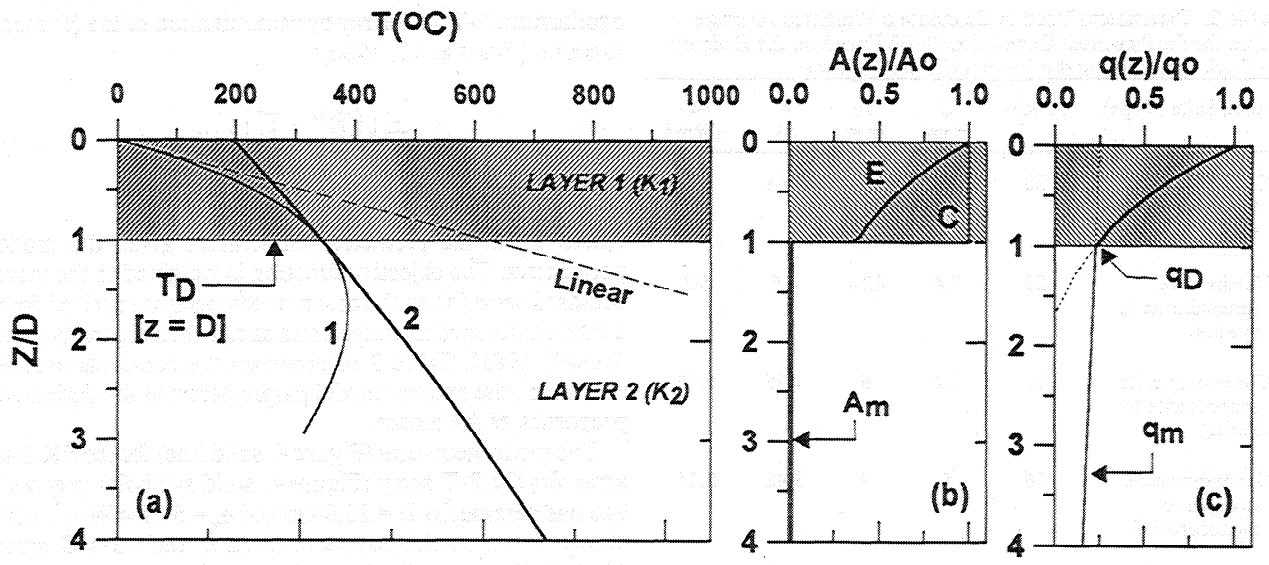

Figure 3. Representation of composite two-layer model for steady state conductive geotherm with radiogenic heat sources, showing (a) geometry of model and temperature distributions (solid lines) for each layer; the geotherm is described by curve 1 for z<**D** and by curve 2 for z>**D**. (b) Model distributions of heat-producing elements (E: exponential **Ao** $e^{-z/D}$ or C: constant **Ao**) in layer 1 relative to the value of surface rocks (**Ao**). Layer 2 has a lower and uniform distribution of heat-producing elements (**Am**). (c) Calculated heat flow at the base of the upper layer (q_D) and in the mantle (q_m) relative to the surface heat flux (q_o).

relate directly to heat budgets in the upper layer, they also reflect the thermal state of the deep mantle.

In summary, by fitting these expressions to the petrological data and solving for q_o and **D**, we are assuming that (1) the P-T array (solid symbols, Figure 2d) is an accurate representation of the P-T conditions in the mantle at the time of kimberlite emplacement, (2) the mantle geotherm for the Slave lithosphere approached a steady state configuration resulting from dominantly conductive processes, (3) lateral variations in the thermal structure of the lithosphere are on a scale that do not compromise this one-dimensional model [e.g., *Jaupart*, 1983], (4) the geotherm was sustained solely by mantle heat flow and by radiogenic heat production in both crustal (layer 1) and mantle (layer 2) rocks, and that (5) the true distribution of radiogenic heat producing elements in the crust is well-approximated by equation (1) [e.g., *Sclater et al.*, 1980; *Cermak and Bodri*, 1989]. Furthermore, in relating the inferred geotherm to present geophysical measurements, we are assuming that the geotherm and crustal configuration have not changed appreciably over the last 172 Ma.

Values of thermal conductivity for upper and lower crust from cool cratonic regimes are expected to vary between 2.37 and 2.64 $Wm^{-1} K^{-1}$, respectively [*Chapman*, 1986]. Following the work of *Schatz & Simmons* [1972] and *Ganguly et al.* [1995] we have assigned a constant value of 2.5 $Wm^{-1} K^{-1}$ for the thermal conductivity of the entire crust (Table 2; layer 1, K_1, z< D). We also used a constant value for the thermal conductivity of layer 2. Our value (K_2) is calculated using the work of *Katsura* [1995] who showed the thermal diffusivity of mantle olivine to be constant at 30 to 60 Kbar pressure over the range of temperatures found in our P-T array. Combining *Katsura*'s [1995] values of thermal diffusivity with average mantle values for density [*Turcotte and Schubert*, 1982] and heat capacity [*Stacey*, 1992], we calculated a range for thermal conductivity of 3.15 $Wm^{-1} K^{-1}$ to 3.28 $Wm^{-1} K^{-1}$ and elected to use a mean value of 3.2 $Wm^{-1} K^{-1}$.

3.2. Calculation of Ao

We estimated an average value of surface radiogenic-heat production (**Ao**) for this region of the Slave craton on the basis of the bedrock geology [*King et al.*, 1990]. Specifically, bulk chemical compositions for outcropping rocks (Table 2) were used to calculate a weighted average value for **Ao** for an area of 14,300 km^2 surrounding the Jericho kimberlite. An average value **Ao** was computed from

$$Ao = \sum_{i=1}^{n} \alpha_i \rho_i \left[\sum_{j=1}^{m} \left(c_j \times h_j \right) \right] \qquad (6)$$

where α_i and ρ_i are the area fraction and density of each of the n rock types and c_j and h_j are the concentrations (ppm) and characteristic decay energies (Table 2) for each of the m radiogenic elements considered. The proportions of rock types comprising the bedrock geology and bulk chemical compositions (Table 2) derive from *Davis* [1991]; the estimates of surface area minimize the abundances of late granitic veins and pegmatites, which intrude virtually all rock types [*W. Davis*, personal communication, 1998]. Consequently, our value of **Ao** (2.16 mWm^{-3}) is a minimum value because granitoids from the Slave craton are generally radiogenically enriched relative to other rock types. Our value is a conservative average for a large area of the crust, which may make it a more appropriate value to use in

Table 2. Parameters Used to Calculate a Weighted Average Value for Surface Heat Generation (HG) Based on the Bedrock Geology Surrounding the Jericho Kimberlite Pipe

Rock Suite (Type)	Area%	U ppm	Th ppm	K %	HG μWm^{-3}
Coghead group (greywacke turbidite)	30	1.7	7	1.68	1.09
Yamba suite (granodiorite to syenite)	23	7.4	42.4	4.5	5.3
Concession suite (granodiorite to diorite)	19	1.4	6	1.76	0.95
Contwoyto suite (tonalite to monzogranite)	16	5	9	3.42	2.24
Siege suite (trondjemite)	6	0	2	1.25	0.26
Volcanic greenstones	3	0.6	5	0.6	0.56
Wishbone suite (tonalite to monzogranite)	2	4	14	2.49	2.24
Olga suite (tonalite)	1	0.6	1	1.16	0.33
Weighted Average (14,300 km^2)		3.38	14.99	2.58	**2.16**

After *Davis* [1991].
Mean density used: 2650 kg m^{-3}; radiometric decay energies in mW kg^{-1}: U = 9.66 x 10^{-2}, Th = 2.65 x 10^{-2}, K = 3.58 x 10^{-5}.

modeling crustal-scale heat flow. Values of **Ao** representing smaller areas (e.g., 1 km by 1 km) will show substantially more variation and are at a scale too small to relate directly to the lithosphere's geotherm.

The value of **Ao** is an objective estimate of present-day heat generation for surface bedrock geology of the Slave craton. Because most of these rocks are older than 2.5 Ga, we have neglected to correct this value for the small decrease in heat production that has occurred since the time of kimberlite emplacement (e.g., 172 Ma). Furthermore, our calculated value of **Ao** and model geometry (Figure 3) neglect the 100-200 m thick sequence of carbonate rocks that covered the bedrock at 172 Ma [*Cookenboo et al.*, 1996] and assume that this thin stratigraphic cover did not significantly affect the paleo-geotherm.

3.3. Model Estimation

Inverting the P-T data (Figure 2d) through equation (5) provides an objective estimate of the parameters $\mathbf{q_o}$ and **D** and the variances and covariances on these two fit parameters based on the quality of the data. Optimal values of the model parameters $\mathbf{q_o}$ and **D** have been derived from the equilibrium P-T data array by minimization of the X^2 merit function [*Press et al.*, 1986]:

$$\chi^2 = \sum_{j=1}^{m} \left[\frac{\left(T_j^{obs} - T_j^{*}\right)}{\sigma_j} \right]^2 \qquad (7)$$

where **T*** is the predicted temperature given the model parameters. The objective function is weighted to the mean standard error (σ) on the observed temperature derived from electron microprobe analysis and sample heterogeneity [e.g., *Russell*, 1981]. Table 3 summarizes the constants used in the model, the optimal model parameters and the derivative properties of the model.

The model geotherm (Figure 4, solid line) for the BK data array fits the P-T array (Figure 4, solid symbols) very well and has parameters **D** = 25.8 km and $\mathbf{q_o}$ = 54.1 mWm^{-2}. Also shown is the model geotherm fitted to the FB-MG array (dashed line) which yields the solution **D**=29.2 km; $\mathbf{q_o}$=56.6. The differences in model parameters are real (10% in **D** and 5% in $\mathbf{q_o}$), and they result because the FB-MG array is offset to lower values of P and T. Furthermore, the FB-MG array contains fewer points at depth (e.g., > 60 Kbar) because the pyroxenite samples fall off the undisturbed portion of the geotherm. Regardless of which thermobarometric method, we predict a high value of surface heat flow and a minimum crustal thickness of > 25 km for the Slave Craton (Table 3).

Table 3. Model Parameters Calculated for Steady State Conductive Geotherm From P-T Data

Parameter	FB-MG	BK
N (P-T points)	21	25
σ_T, °C	25	25
K_1, $Wm^{-1}K^{-1}$	2.5	2.5
K_2, $Wm^{-1}K^{-1}$	3.2	3.2
Ao, μWm^{-3}	2.16	2.16
Am, μWm^{-3}	0.04	0.04
q_o, mWm^{-2}	56.6	54.1
D, km	29.2	25.8
χ^2	13.7	31.3
$(dT/dz)_{MOHO}$, °C/km	6.69 - 5.23	7.55 - 5.90
q_{MOHO}, mWm^{-2} (Z=D)	16.73	18.87
$(dT/dz)_m$, °C/km (100-200 km)	4.34 - 3.09	4.97 - 3.72
q_m, mWm^{-2} (100-200 km)	13.90 - 9.90	15.91 - 11.91

Parameters include the following: 1 sigma estimate of uncertainty on xenolith temperatures (σ_T); chi-square statistic on minimization (χ^2); temperature gradients (dT/dz) for layer 1 and layer 2 at z=D (MOHO); heat flow (q) at depths of z=D; and heat flow and gradients in the mantle (m).

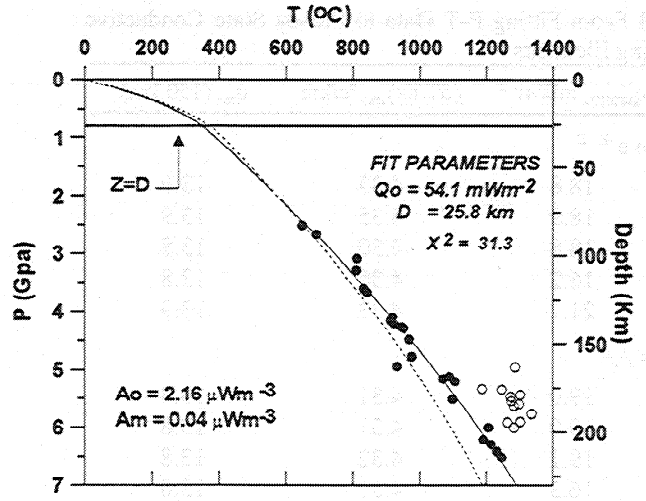

Figure 4. Best fit geotherm is compared to distribution of P-T data (Table 1). Dashed line denotes the fit to P-T array generated by *Finnerty and Boyd* [1987] used in conjunction with *MacGregor* [1974]. Only data shown as solid symbols are used in inversion (see text).

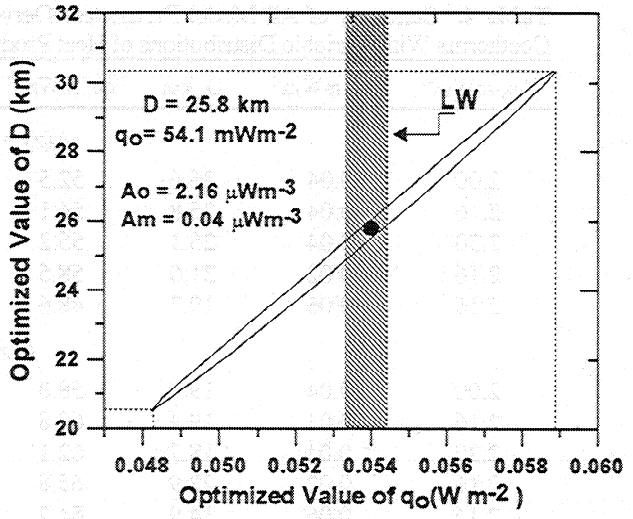

Figure 6. Confidence limits (3 s) on the optimal fit parameters $\mathbf{q_o}$ and **D** showing the degree of correlation between the two parameters and the maximum range of permissible values (dotted lines) given the distribution of P-T data. Field-measured value of surface heat flow from *Lewis and Wang* [1992] is shown by shaded pattern (see text).

The quality of the fit to the data is shown in Figures 5 and 6. Figure 5 shows the distribution of residuals (T_{obs} - T_{model}) as a function of the input parameters. Residuals are 50°C or less and are symmetrically distributed where plotted against the input data (P and T). We found no obvious explanation for the single outlier (> 50 °C). One attribute of using the X^2 merit function is that confidence limits can be placed on the optimal solution [e.g., *Press et al.*, 1986]. Figure 6 shows the solution [**D**, $\mathbf{q_o}$] and the 3 s confidence limits on the fit parameters; the ellipse quantitatively shows the degree of correlation between the two parameters and constrains the maximum range of permissible values given the observed distribution of P-T data. At the 3 s confidence level, the bounds on **D** are 20.6 to 30.4 km and on $\mathbf{q_o}$ are 48.3 to 58.9 mWm^{-2}.

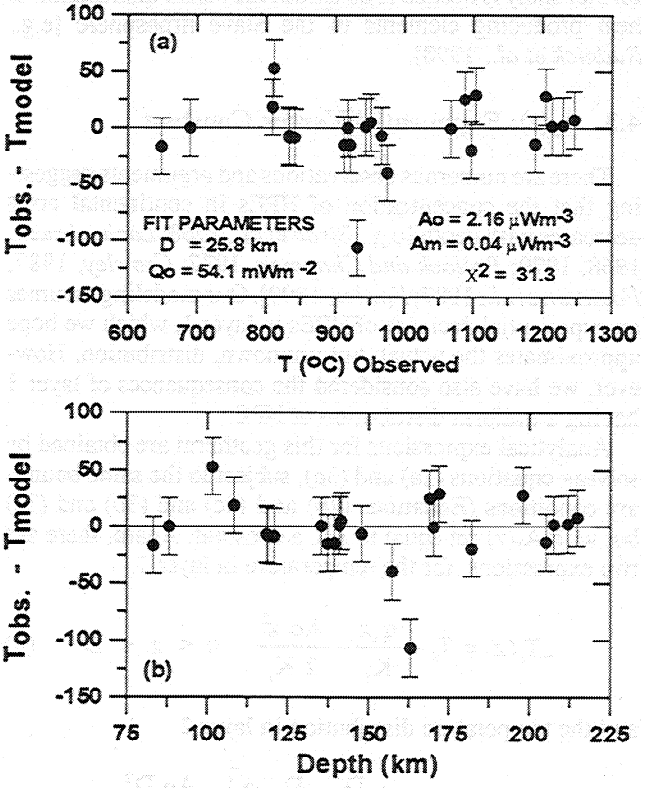

Figure 5. Distribution of residuals on temperature (observed-predicted) plotted as a function of T(°C) and depth (pressure). Residuals appear to be distributed randomly and, except for a single datum, are 50 °C or less.

4. Heat Production Considerations

The most important assumptions made in calculating the model geotherm concern the nature of heat producing elements in layer 1 and layer 2. Our assumptions are three-fold: (1) that the value of **Ao** (2.16 mWm^{-3}) is a fair estimate of surface heat production, (2) that mantle heat production is adequately described by a uniform value of 0.04 mWm^{-3}, and (3) that the distribution of HPE in layer 1 decreases exponentially with depth. Prior to analyzing the implications of our preferred results (Figure 4, Table 3) for the Slave lithosphere, we examine some of the consequences of these assumptions.

4.1. Values of Ao

The model geotherm assumes an exponential decrease in HPE within layer 1. The actual amount of radiogenic heat generation at depth is predicated by the value of heat production for surface crustal rocks (e.g., **Ao**). We have argued that a value of 2.16 mWm^{-3} is reasonable (see above); however, we have also explored the sensitivity of our model results to variations in **Ao**. Specifically, we have modeled the system for values of **Ao** of 2.0 and 2.3 mWm^{-3}, while

Table 4. Summary of All Model Parameters Derived From Fitting P-T Data to Steady State Conductive Geotherms With Variable Distributions of Heat Producing Elements

Ao, mWm^{-3}	Am, mWm^{-3}	D, km	qo, mWm^{-2}	q_{MOHO}, mWm^{-2}	$(dT/dz)_{150}$, °c/km	q_m, (150 km)
			$A(z) = Ao\ e^{-Z/D}$			
2.00	0.04	26.6	52.5	18.8	4.33	13.9
2.16	0.04	25.8	54.1	18.9	4.35	13.9
2.30	0.04	25.1	55.2	18.8	4.30	13.8
2.16	0.02	31.0	58.5	16.2	4.30	13.8
2.16	0.06	19.7	48.6	21.7	4.33	13.9
			$A(z) = Ao$			
2.00	0.04	19.9	58.8	19.0	4.31	13.8
2.16	0.04	19.4	60.8	19.0	4.31	13.8
2.30	0.04	18.7	62.1	19.1	4.32	13.8
2.16	0.02	22.9	65.8	16.3	4.31	13.8
2.16	0.06	14.9	54.2	22.0	4.33	13.9

maintaining all other values constant. Results are tabulated in Table 4 and shown in Figure 7a.

Figure 7a shows our preferred solution (i.e., Figures 4 and 6) compared to solutions arising from lower and higher assumed values of **Ao**. All solutions are shown with their associated 3 s confidence limits; clearly, the nature of correlation between the parameters $\mathbf{q_o}$ and **D** remains virtually constant. Variations in **Ao** generate unique but overlapping solutions. Lower values of **Ao** require a thicker crust (27 km) and lower surface heat flow (52.5 mWm^{-2}). Higher values of **Ao** demand a slightly thinner crust (25 km) and higher values of $\mathbf{q_o}$ (55.2 mWm^{-2}). Second, where compared to the measured surface heat flow for the Slave craton from *Lewis and Wang* [1992], all three solutions must be considered reasonable. Lastly, the model solution appears to be relatively insensitive to reasonable variations in **Ao**. In this particular example, a 15% variation in **Ao** generated a 5% and 10% change in $\mathbf{q_o}$ and **D**, respectively (Table 4).

4.2. Values of Am

Our preferred solution uses an intermediate value of 0.04 mWm^{-3}, for heat production in the lithospheric mantle (**Am**). Values reported for depleted mantle commonly are as low as 0.02 mWm^{-3} and *Rudnick et al.* [1998] showed that values exceeding 0.06 mWm^{-3} tend to produce unreasonable geotherms. Therefore, in order to gauge the sensitivity of our modeling to variations in radiogenic heat production in the lithosphere, we have used limiting values of **Am** of 0.02 and 0.06 mWm^{-3}. Results of this modeling are illustrated in Figure 7b and tabulated in Table 4.

All three solutions (including the preferred model) are shown on Figure 7b with their respective 3 s confidence envelopes. A comparison of Figure 7a to 7b, however, shows that values of **Am** affect the model geotherm in a markedly different way than does **Ao**. The solution parameters $\mathbf{q_o}$ and **D** remain highly correlated, but the confidence regions around the solution increase slightly with increasing **Am**. Furthermore, variations in **Am** generate unique solutions that have 50% or less overlap. Increased values of **Am** require a thinner crust (26 to 20 km) and lower values of surface heat flow (54 to 49 mWm^{-2}). The single field measurement of $\mathbf{q_o}$ [*Lewis and Wang*, 1992] agrees best with an intermediate value for **Am** and is inconsistent with the lowest value (0.02). In summary, the model solutions are very sensitive to variations in **Am**. The range of values for radiogenic heat production used here are not extreme given the diverse nature of the Slave lithosphere [e.g., *Kopylova et al.* 1998a, 1998b], but cause a 18% variation in $\mathbf{q_o}$ and a 40% change in **D** (Table 4). These results suggest that further study is needed to constrain the actual distribution of heat producing elements in the Slave lithosphere [e.g., *Rudnick et al.*, 1998].

4.3. $A_1(z)$: Exponential Versus Constant

There are numerous observations and arguments suggesting that the concentration of HPEs in continental crust decreases with depth [e.g., *Birch et al.*, 1968; *Lachenbruch*, 1968, 1970; *Pollack and Chapman*, 1977; *Crowley*, 1987; *Fountain et al.*, 1987; *Fowler*, 1990]. Our modeling assumes an exponential decrease of HPEs in layer 1, which we hope approximates the actual, but unknown, distribution. However, we have also considered the consequences of layer 1 having a uniform distribution of HPE.

Analytical expressions for this geotherm are obtained by solving equations (2a) and (3a), subject to the same boundary conditions (Equations (2b) and (2c) and (3b) and (3c) but with $A_1(z)$ set equal to **Ao**, a constant. Again, there are two expressions, for the temperature in layer 1

$$T_1(z) = T_s + \frac{q_o z}{K_1} - \frac{Ao\ z^2}{2\ K_1} \qquad 0 < z < D \qquad (8)$$

and the temperature distribution in layer 2

$$T_2(z) = T_s + q_o\left[\frac{D}{K_1} - \frac{D-z}{K_2}\right] - \frac{Ao\ D^2}{2\ K_1} \qquad (9)$$

$$+ \frac{Ao\ D\ (D-z)}{K_2} - \frac{Am\ (D-z)^2}{2\ K_2} \qquad D < z < \infty.$$

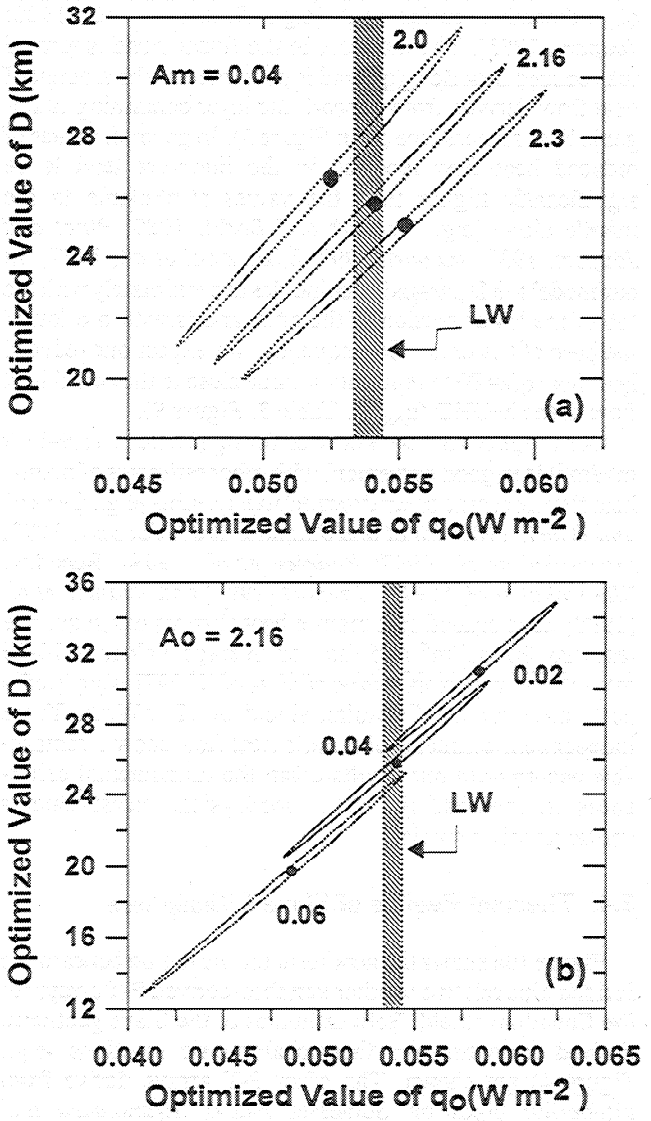

Figure 7. Sensitivity (shown as 3 s confidence limits) of model parameters q_o and **D** to variations in values of (a) surface heat production (**Ao**) and (b) mantle heat production (**Am**). Pattern labeled LW is the value of surface heat flow measured by *Lewis and Wang* [1992].

Fitting these equations to the thermobarometric data, we obtained a best fit solution (**Ao** = 2.16 and **Am** = 0.04) that describes the P-T array well and has parameters **D** = 19.4 km and q_o = 60.8 mWm^{-2} (Figure 8). We also have explored the sensitivity of this model to changes in the variables **Ao** and **Am**. The results are compiled in Table 4 and illustrated in Figure 8, in the same manner as used in Figure 7.

The best fit solutions span values of q_o and **D** from 54 to 66 mWm^{-2} and from 15 to 23 km, respectively. In general, a uniform distribution of HPEs in the crust requires substantially higher surface heat flow and thinner crust. The solution regions shown in Figure 8, outlined by 3 s confidence limits, show the same correlation patterns as seen in Figure 7. Furthermore, variations in **Ao** and **Am** generate roughly the same shifts in optimal parameters. The only solution that brackets the field measured value of surface heat flow [*Lewis and Wang*, 1992] is the one that uses a high value of mantle heat production (0.06). All other solutions require model values of q_o close to 60 mWm^{-2}. In order to obtain a model value for q_o of 53-54 mWm^{-2} by reducing the amount of HPEs in layer 1, **Ao** would need to be as low as 1.5 mWm^{-3}.

5. Discussion

5.1. Surface Heat Flow (q_o)

Having established a value for **Ao**, a priori, we have estimated model values of surface heat flow (q_o) and the apparent depth-scale parameter **D**. Our value of q_o (54.1 mWm^{-2}) agrees well with heat flow measurements reported by *Lewis and Wang* [1992] for the southwest Slave craton (e.g., 53.3 - 54.4 mWm^{-2}) and *Beck and Sass* [1966] for the Muskox Intrusion (54.92 ± 4.2 mWm^{-2}). The latter measurement is located immediately northeast of Jericho; it is situated off the craton but within the limits of reworked Archean crust [e.g., *Hoffman*, 1989]. The only other relevant measurement of surface heat flow appears to be a measurement at Resolute Bay (52.3 mWm^{-2} [*Lachenbruch*, 1957]) which is situated on Proterozoic basement, north of the Slave craton.

Our estimate of q_o is considerably higher than previous values derived for the Slave craton from studies of mantle xenoliths [e.g., *Boyd and Canil*, 1997; *MacKenzie and Canil*, 1997; *Pearson et al.*, 1998]. Our value of q_o is also substantially larger than the value of 42-44 mWm^{-2} estimated by *Kjarsgaard and Petersen* [1992] in their study of xenoliths from the Somerset Island kimberlite. Somerset Island is close to Resolute Bay where *Lachenbruch* [1957] measured values of q_o in excess of 50 mWm^{-2}. Our results suggest that the Slave craton is characterized by high

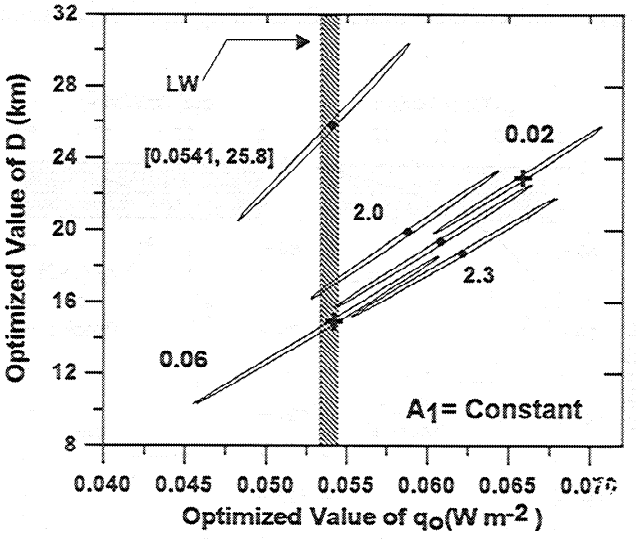

Figure 8. Comparison of solution that uses an exponential distribution of HPE (**Ao** $e^{-z/D}$) in layer 1 to results for model with constant HPE (**Ao**). Sensitivity analysis of model parameters to variations in values of **Ao** and **Am** is also shown. Surface heat flow measurement (LW) shown for comparison (as in Figure 7).

surface heat flow relative to the mean values of heat flow cited for Archean and Proterozoic provinces (e.g.,41 mWm^{-2} [*Nyblade and Pollack*, 1993; *Jaupart*, 1997]). It is, however, well within the range of values generally reported for continental heat flow provinces.

5.2. D Parameter

Our estimate of the D parameter (25.8 km) for the Slave craton is constrained to lie between values of 21 and 30 km. The most reliable geophysical data for the crustal portions of the Slave lithosphere derive from the interpreted seismic sections of *Clowes* [1997]. These seismic data show that crust beneath the southern Slave Craton is between 32 and 36 km thick [e.g., *Clowes*, 1997; *Bostock and Cassidy*, 1997]. Our value of **D** is slightly less than the thickness of the entire crustal section but is equivalent to the combined thickness of upper and middle crust where the majority of heat producing elements are expected to be concentrated.

5.3. MOHO (q_{MOHO}) and Mantle (q_m) Heat Flow

Figure 9 shows the geothermal gradient and heat flow for the Slave lithosphere implied by our model. In layer 1 the temperature gradient decreases from 22 °C km^{-1} at the surface to 7.6 °C at the MOHO (Figure 9a). Below the MOHO (layer 2) the temperature gradient decreases at a near constant rate from 5 to 3.7 °C km^{-1} between 100 and 200 km depth.

Heat flow in the crustal layer decreases from 54 mWm^{-2} (q_o) to 18.9 mWm^{-2} at the MOHO (q_{MOHO}). Layer 2 has a near linear heat flow profile. Between 100 and 200 km mantle heat flow (q_m) has values of between 15.9 and 11.9 mWm^{-2}.

In studies involving field measurements of **Ao** and q_o, data for individual heat flow provinces commonly define unique linear trends [e.g., *Birch et al.*, 1968; *Lachenbruch*, 1970; *Fountain et al.*, 1987]. The slope of the linear trend has the units of meters and defines the apparent depth-scale of radioactive enrichment [e.g., *Sclater et al.*, 1980; *Jaupart*, 1983]. The intercept to the linear trend is termed the reduced heat flow (q_r) and is construed as the amount of heat flow derived from beneath the layer containing radiogenic heat sources (see q_D in Figure 3). In general, values of reduced heat flow reported in the literature tend to be significantly higher than the values attributable to the mantle alone [e.g., *Cermak and Bodri*, 1989; *Pinet and Jaupart*, 1987; *Jaupart*, 1997; *Mareschal et al.*, 1997]. In our model the **D** parameter coincides approximately with the top of the lower portion of the crust and is within 6 km of the base of the crust. Consequently, we expect our reduced heat flow q(z=**D**) to represent a value close to the actual heat flow at the MOHO (q_{MOHO}, Table 3, Figure 9).

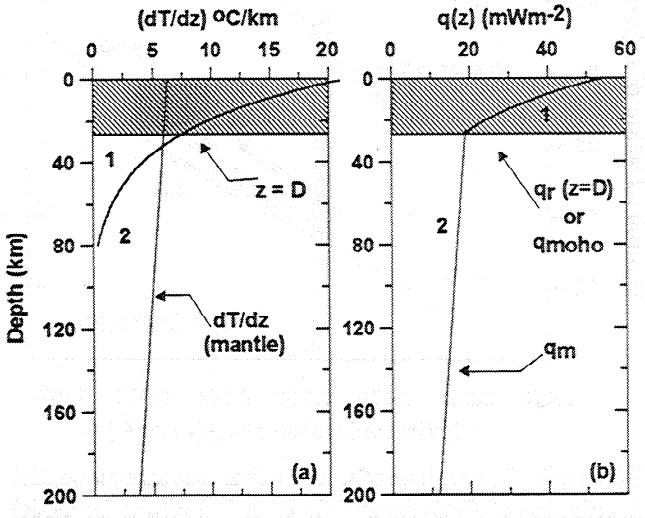

Figure 9. Model results shown as (a) geothermal gradients (°C/Km) in layers 1 and 2 and (b) calculated heat flow (mWm^{-2}) in same layers (see text).

Our range of values calculated for q_m (Table 3, 15.9-11.9 mWm^{-2}) is in good agreement with other estimates of mantle heat flow for some other Precambrian terrains [e.g., *Cermak and Bodri*, 1989; *Pinet and Jaupart*, 1987; *Jaupart*, 1997; *Mareschal et al.*, 1997; *Rudnick et al.*, 1998]. Recently, *Mareschal et al.* [1997], *Jaupart* [1997] and *Rudnick et al.* [1998] have argued that mantle heat flow values should be less than 20 mWm^{-2} and that, on average, values of 10-15 mWm^{-2} are expected. *Mareschal et al.* [1997] suggested a best value for the Canadian shield of 12 mWm^{-2}. These independent estimates of mantle heat flow show a remarkable accord with our results given the fundamental differences in methodology (e.g., geophysical measurements versus xenolith studies).

5.4. Thermal Regime of Slave Lithosphere

Figure 10a shows the geotherm for the region beneath the Jericho pipe relative to other xenolith-derived P-T arrays for the Canadian shield. Both estimates of the Slave geotherm derived from the two thermobarometric solutions (e.g., Figure 4) are shown. The other P-T arrays derive from kimberlite pipes on Somerset Island [*Kjarsgaard and Peterson*, 1992], near Lac de Gras [*Boyd and Canil*, 1997; *MacKenzie and Canil*, 1997; *Pearson et al.*, 1998] and at Kirkland Lake [*Meyer et al.*, 1994; *Schulze*,1996].

The thermal state of the Jericho mantle is similar to that reported from other kimberlite bodies in the central Slave province (compare curves 4, 5, and 6, Figure 10a). P-T arrays derived from the Grizzly [*Boyd and Canil*, 1997], Torrie [*MacKenzie and Canil*, 1997] and Lac de Gras [*Pearson et al.*, 1998] pipes more or less coincide with our geotherm (Figure 10a). Relative to P-T arrays for other North American kimberlite occurrences (e.g., curves 1, 2, and 3, Figure 10a), the upper mantle beneath the Slave Craton is cool. Specifically, the P-T arrays for lithosphere underlying the northern Proterozoic terrains of the Canadian Shield (curve 1, Somerset Island) and the Superior province (curves 2 and 3, Kirkland Lake) show the Slave lithosphere to be measurably cooler. This underlies the fact that the high values of surface heat flow that characterize the Slave Craton result from the Slave crustal rocks being enriched in HPEs.

Figure 10b compares our model geotherms for the north central Slave craton (A) to xenolith-derived P-T arrays from other Archean cratons and from continental basaltic provinces. Representations of the lithosphere for these different

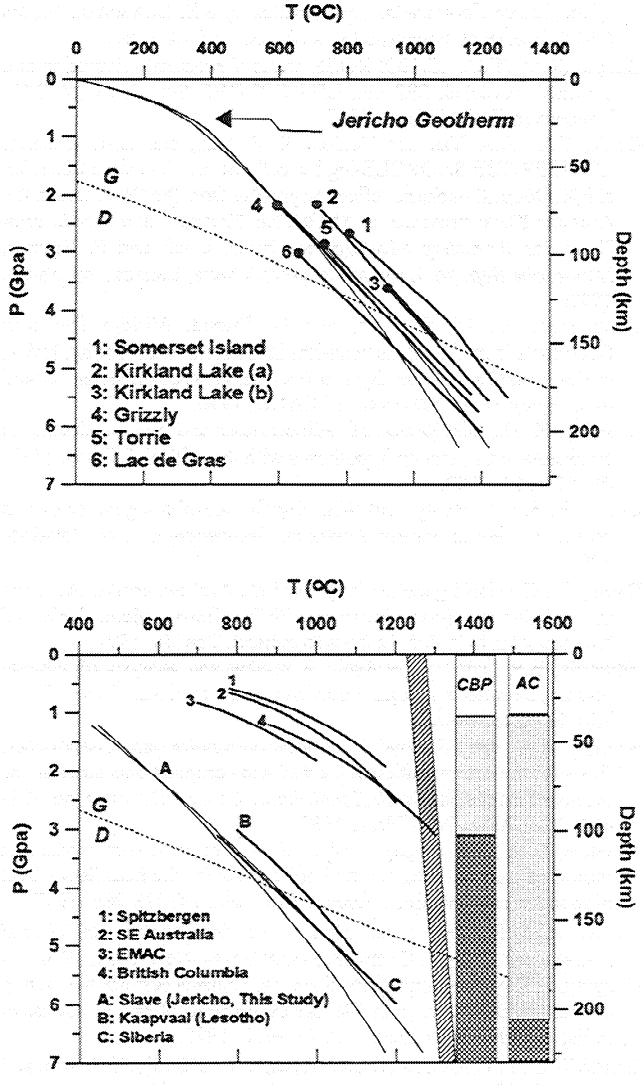

Figure 10. Comparison of this work to studies of other xenolith suites. Upper panel compares our geotherms (Figure 4) for the lithosphere beneath Jericho pipe to P-T data for xenoliths from other North American kimberlite occurrences. Data are from (1) *Kjarsgaard and Peterson* [1992], (2) *Schulze* [1996], (3) *Meyer et al.*, [1994], (4) *Boyd and Canil* [1997], (5) *MacKenzie and Canil* [1997] and (6) *Pearson et al.* [1998]. Lower panel compares geotherm for the north central Slave craton (curve A) to P-T data on xenoliths from other Archean cratons (AC, curves B-C) and from continental basaltic provinces (CBP, curves 1-4). P-T data and corresponding sources are (curve A) this study (BK and FB-MG), (curve B) Northern Lesotho, Southern Africa [*Finnerty and Boyd*, 1987], and (curve C) lower temperature limit of Daldyn kimberlite field, Siberia [*Griffin et al.*, 1996; *Boyd et al.*, 1997], and (1) Spitsbergen [*Amundsen et al.*, 1987], (2) South Eastern Australia [*O'Reilly and Griffin*, 1985], (3) EMAC [e.g., *O'Reilly and Griffin*, 1996], (4) Big Timothy Mountain and Jacques Lake, British Columbia [*Ross*, 1983]. Right side of lower panel compares geometry of mantle adiabat [e.g., *Akaogi et al.* 1989] to cross sections for AC and CBP showing relative distributions of crust (no pattern), conductive upper mantle (light shading), and convecting mantle (cross-hatched).

portions of the earth are shown schematically on the right side of the panel (Figure 10b). The P-T distributions of xenoliths derived from continental basaltic provinces (CBP) show substantially hotter lithosphere, reflecting that in these regions conductive geotherms are likely disturbed by convective processes [*O'Reilly and Griffin*, 1985] and the depths to the convecting mantle are shallower. A more pertinent comparison is between our geotherms and those established for other Archean cratons. Figure 10b shows P-T arrays for both South Africa [e.g., *Finnerty and Boyd*, 1987] and Siberia [e.g., *Griffin et al.*, 1996; *Boyd et al.*, 1997] which were calculated using the same thermobarometric solutions as used in this study. The lithosphere beneath Jericho, and the Slave Craton in general (Figure 10a), is clearly cooler than that underlying the Kaapvaal. The data for Siberia define a P-T array with abundant scatter probably indicating that the xenoliths are not part of a single well equilibrated geotherm [*Boyd et al.*, 1997]. The Siberian geotherm is represented in Figure 10b by a single line marking the lower temperature limit of the P-T data and roughly coincides with the geotherm derived for the Slave Craton.

6. Conclusions

Our model is a composite, two-layer, one-dimensional, analytical model for a steady state conductive geotherm with layer specific distributions of radiogenic heat sources. We have fit this model to P-T data on xenoliths from the Jericho kimberlite in order to constrain the values of $\mathbf{q_o}$ and **D** for the north central Slave craton at the time of kimberlite magmatism.

Our results are consistent with a surface heat flow of 54.1 mWm^{-2} and a D parameter of 25.8 km and are applicable to a depth of 200 km, where the P-T array for mantle xenoliths is disturbed (Figures 2d and 4). Our value of $\mathbf{q_o}$ is substantially higher than estimated from previous studies of Slave mantle xenoliths. The high surface heat flow derives from the fact that crustal rocks of the Slave craton are highly radiogenic ($\mathbf{A_o}$ = 2.16 μWm^{-3}). Our estimate of **D** is roughly equal to the thickness of the upper and middle crust as established for the southern Slave [*Clowes*, 1997; *Bostock* and *Cassidy*, 1997]. Conversely, our results may point to a slightly thinner crust underlying the northern Slave craton.

There are two main merits to our approach. First, we have achieved a better fit to the petrological data than is commonly achieved by matching thermobarometric data to standardized steady state geotherms. Our fit of the geotherm to the available P-T data produces an even distribution of residuals that is fully consistent with petrologic uncertainties. On the basis that our fitted geotherm is a better representation of the data, we suggest that, in all probability, we have produced a more accurate picture of the thermal state of the Slave lithosphere (e.g., Figure 9). Lastly, the results of our model agree well with the only surface heat flow measurements available for the Slave craton, albeit a single measurement from the southern portion of the craton.

Our modeling, and work by *Rudnick et al.* [1998], clearly shows that P-T array data on mantle xenoliths are permissive of a wide range of values for crustal thickness and heat-producing properties of the crust. A second attribute of our

approach therefore is that inversion of the petrological data provides an objective evaluation of parameters related to the geophysical structure of the lithosphere. Our modeling quantifies the correlation between $\mathbf{q_o}$ and **D** and restricts the range of permissive values for these two important parameters.

We elected to fit a simple, yet realistic, geophysical model for cratonic geotherms to the petrological data. From the perspective of interpreting the fit, the simple model is preferred because of the small number of adjustable parameters. Clearly, more complicated geophysical models could be fit to the same data; however, the uncertainties on each additional fit parameter would increase accordingly, as would the nonuniqueness of the solutions.

Acknowledgements. This research was originally funded by an NSERC Industrially Oriented Research partnership between Canamera Geological Ltd and the Igneous Petrology Laboratory at UBC. We are indebted to Lytton Minerals Ltd for material and continued financial support. Our research was facilitated by Bill Davis, who gave us access to unpublished data. We also benefitted from discussions with Art Calderwood, Bill Davis and, especially, Trevor Lewis. Finally, thorough and critical reviews by Dante Canil, Paul Morgan, and Roberta Rudnick helped improve both the clarity of our arguments and the thoroughness of our sensitivity analysis. This does not imply agreement on all issues. MATLAB scripts for modeling P-T arrays are available via e-mail (russell@perseus.geology.ubc.ca).

References

Akaogi, M., E. Ito, and A. Navrotsky, Olivine-modified spinel-spinel transitions in the system Mg_2SiO_4-Fe_2SiO_4: Calorimetric measurements, thermochemical calculation, and geophysical application, *J. Geophys. Res., 94*, 15671-15685, 1989.

Amundsen, H.E.F., W.L. Griffin, and S.Y. O'Reilly, The lower crust and upper mantle beneath northwestern Spitsbergen: Evidence from xenoliths and geophysics, *Tectonophys., 139*, 169-185, 1987.

Beck, A.E., and J.H. Sass, A preliminary value of heat flow at the Muskox Intrusion near Coppermine, N.W.T., Canada, *Earth Planet. Sci. Lett., 1*, 123-129, 1966.

Birch, F., R.F. Roy, and E.R. Decker, Heat flow and thermal history in New England and New York, in *Studies of Appalachian Geology*, edited by E. An-Zen, pp. 437-451, John Wiley, New York, 1968.

Bostock, M. G., and J.F. Cassidy, Upper mantle stratigraphy beneath the southern Slave Craton, *Can. J. Earth Sci., 34*, 577-587, 1997.

Boyd F.R., and D. Canil, Peridotite xenoliths from the Slave Craton, Northwest Territories, Paper presented at the 7th Goldschmidt Conference, Geochem. Soc., Tucson, Ariz., June 2-6, 1997.

Boyd, F.R., N.P. Pokhilenko, D.G. Pearson, S.A. Metzman, N.V. Sobolev, and L.W. Finger, Compositions of the Siberian cratonic mantle: Evidence from Udachnaya peridotite xenoliths, *Contrib. Mineral. Petrol., 128*, 228-246, 1997.

Brey G.P., and T. Köhler, Geothermobarometry in four-phase lherzolites, II, New thermobarometers, and practical assessment of existing thermobarometers, *J. Petrol., 31*, 1353-1378, 1990.

Bussod, G.Y.A., and D.R. Williams, Thermal and kinematic model of the southern Rio Grande rift: Inferences from crustal and mantle xenoliths from Kilbourne Hole, New Mexico, *Tectonophys., 197*, 373-389, 1991.

Cermak, V., and L. Bodri, On the vertical distribution of radiogenic heat production in the continental crust and the estimated MOHO heat flow, *J. Geophys. Res., 94*, 235-242, 1989.

Cermak, V., L. Bodri, and L. Rybach, Radioactive heat production in the continental crust and its depth dependence, in *Terrestrial Heat Flow and the Lithosphere Structure*, edited by V. Cermak and L. Rybach, pp. 23-69, Springer Verlag, New York, 1991.

Chapman, D.S., Thermal gradients in the continental crust, in *The Nature of the Lower Continental Crust*, edited by J.B. Dawson et. al., pp. 63-70, Blackwell Scientific Publications, Oxford, 1986.

Clowes, R.M. (Ed.), LITHOPROBE phase V proposal - Evolution of a continent revealed, 292 pp., LITHOPROBE Sec., Univ. of B.C., Vancouver, B. C.,Canada, 1997.

Cook, F.A., A.J. Van der Velden, K.W. Hall, and B.R. Roberts, LITHOPROBE SNORCLE-ing beneath the northwestern Canadian shield: Deep lithospheric reflection profiles from the Cordillera to the Archean Slave province, in *SNORCLE Transect and Cordilleran Tectonics Workshop Meeting*, ed. by F. Cook and P. Erdmer, *Lithoprobe Rep. 56*, Univ. of Calgary, Alberta, Canada, pp. 58-62, 1997.

Cookenboo, H., M. Orchard, and D. Daoud, Middle Devonian Conodonts from limestone xenoliths in the Jericho kimberlite, NWT, in *Northwest Territories Exploration Overview*, compiled and edited by E. Igboji et al., Yellowknife DIAND, 1996.

Crowley, K. D., Distribution of radioelements and heat production in continental crust, testing hypotheses with the drill, *EoS Trans. AGU, 68*, 553-558, 1987.

Cull, J.P., S.Y. O'Reilly, and W.L. Griffin, Xenoliths geotherms and crustal models in eastern Australia, *Tectonophys., 192*, 359-366, 1991.

Davis, W., Granitoid geochemistry and Late Archean crustal evolution in the Central Slave Province, Ph.D. thesis, Mem. Univ. of Newfoundland, St. John's, Newfoundland, Canada, 1991.

Edwards, B.R., and J.K. Russell, A review and analysis of mineral dissolution rates in naturally occurring silicate melts, *Chem. Geol., 130*, 233-245, 1996.

Finnerty, A.A., and J.J. Boyd, Thermobarometry for garnet peridotites: Basis for the determination of thermal and compositional structure of the upper mantle, in *Mantle Xenoliths*, edited by P.H. Nixon, pp. 381-402, John Wiley, New York, 1987.

Fountain, D.M., K.P. Furlong, and M.H. Salisbury, A heat production model of a shield area and its implications for the heat flow - heat production relationship, *Geophys. Res. Lett., 14*, 283-286, 1987.

Fowler, C.M.R. *The Solid Earth: An Introduction to Global Geophysics*, 472 pp., Cambridge Univ. Press, New York, 1990.

Ganguly, J., R.N. Singh, and D.N. Ramana, Thermal perturbation during charnokitization and granulite facies metamorphism in southern India, *J. Metamorph. Geol., 13*, 419-430, 1995.

Griffin W.L., F.V. Kaminsky, C.G. Ryan, S.Y. O'Reilly, T.T. Win, and I.P. Ilupin, Thermal state and composition of the lithospheric mantle beneath the Daldyn kimberlite field, Yakutia, *Tectonophys., 262*, 19-33, 1996.

Grotzinger, J., and L. Royden, Elastic strength of the Slave craton at 1.9 Gyr and implications for the thermal evolution of the continents, *Nature, 347*, 64-66, 1990.

Heaman L.M., R.A. Creaser, and H.O. Cookenboo, Zircons from eclogite in the Jericho kimberlite pipe, northern Canada: Evidence for Proterozoic high pressure metamorphism beneath the Slave Province, *Proceedings of the 7th International Kimberlite Conference*, Cape Town Univ., Cape Town, S. Africa, April 1998, pp. 325-327, 1998.

Hoffman, P., Precambrian geology and tectonic history of North America, in *The Geology of North America: An Overview*, edited by A.W. Bally and A.R. Palmer, pp. 447-512, Geol. Soc. of Am., Boulder, Colo., 1989.

Jaupart, C., Horizontal heat transfer due to radioactivity contrasts: Causes and consequences of the linear heat flow relation, *Geophys. J.R. Astron. Soc., 75*, 411-435, 1983.

Jaupart, C., Thermal structure of the continental lithosphere from heat flow studies, *Paper presented at MIT-Harvard Workshop on Continental Roots*, Harvard Univ., Boston, MA, USA, Oct. 10 - 13, 1997.

Katsura, T., Thermal diffusivity of olivine under upper mantle conditions, *Geophys. J. Int., 122*, 63-69, 1995.

King, J.E., W. Davis, C. Relf, and T. Van Nostrand, Geology of the Contwoyto-Nose Lakes map area, central Slave Province, District of MacKenzie, N.W.T., in *Current Research, Part C, Pap. 90-1c*, pp. 177-187, Geol. Surv. Can., 1990.

Kjarsgaard, B.A., Slave Province kimberlites, NWT, in *Searching for Diamonds in Canada*, edited by A.N. LeCheminant, et. al., *Open File Rep. 3228*, pp. 55-60, Geol Surv. Can., 1996.

Kjarsgaard B.A., and T.D. Petersen, Kimberlite-derived ultramafic xenoliths from the diamond stability field: A new Cretaceous geotherm for Somerset Island, Northwest Territories, in *Current Research, Part B, Pap. 92-1B*, pp. 1-6, Geol Surv. Can., 1992.

Kopylova, M.G., J.K. Russell, and H. Cookenboo, Upper-mantle stratigraphy of the Slave craton, Canada: Insights into a new kimberlite province, *Geology*, *26*, 315-318, 1998a.

Kopylova, M.G., J.K. Russell, and H. Cookenboo, Petrology of peridotite and pyroxenite xenoliths from the Jericho kimberlite: Implications for thermal state of the mantle beneath the Slave craton, northern Canada. *J. Petrol.*, *40*, 79-104, 1998b.

Lachenbruch, A.H., Thermal effects of the ocean on permafrost, *Geol. Soc. Am. Bull.*, *68*, 1515-1529, 1957.

Lachenbruch, A.H., Preliminary geothermal model of the Sierra Nevada, *J. Geophys. Res.*, *73*, 6977-6989, 1968.

Lachenbruch, A.H., Crustal temperature and heat production: Implications of the linear heat flow relation, *J. Geophys. Res.*, *75*, 3291-3300, 1970.

Lewis, T.J., and K. Wang, Influence of terrain on bedrock temperatures, *Global Planet. Change*, *98*, 87-100, 1992.

MacGregor, I.D., The system MgO-Al_2O_3-SiO_2: Solubility of Al_2O_3 in enstatite for spinel and garnet peridotite compositions, *Am. Mineral.*, *59*, 110-119, 1974.

MacKenzie, J.M., and D. Canil, Petrologic nature of the lower crust and upper mantle beneath the Archean Slave Province, NWT, Canada, in *SNORCLE Transect and Cordilleran Tectonics Workshop Meeting*, edited by F. Cook and P. Erdmer, *Lithoprobe Rep. 56*, pp. 223-224, Univ. of Calgary, Alberta, Canada, 1997.

Mareschal, J.C., C. Jaupart, A. Davaille, and L. Guillou-Frottier, Mantle heat flow and lithospheric thickness in the Canadian shield, *EoS Trans. AGU, 78*, Fall Meet. Suppl., F698, 1997.

Meyer, H.O.A., M.A. Waldman, and B.L. Garwood, Mantle xenoliths from kimberlite near Kirkland Lake, Ontario, *Can. Mineral.*, *32*, 295-306, 1994.

Nyblade, A.A., and H.N. Pollack, A global analysis of heat flow from Precambrian terrains: Implications for the thermal structure of Archean and Proterozoic lithosphere, *J. Geophys. Res.*, *98*, 12207-12218, 1993.

O'Reilly, S.Y., and W.L. Griffin, A xenolith-derived geotherm for southeastern Australia and its geophysical implications, *Tectonophys.*, *111*, 41-63, 1985.

O'Reilly, S.Y., and W.L. Griffin, 4-D lithosphere mapping: Methodology and examples, *Tectonophys.*, *262*, 3-18, 1996.

Padgham, W.A., and W.K. Fyson, The Slave Province: A distinct craton, *Can. J. Earth Sci.*, *29*, 2072-2086, 1992.

Pearson, N.J., W.L. Griffin, B.J. Doyle, S.Y. O'Reilly, E. van Achterbergh, and K. Kivi, Xenoliths from kimberlite pipes of the Lac de Gras area, Slave Craton, Canada, *Proceedings of the 7th International Kimberlite Conference*, Cape Town Univ., Cape Town, S. Africa, April 1998, pp. 670-672, 1998.

Pell, J.A., Kimberlites in the Slave Craton, Northwest Territories, Canada, *Geosci. Can.*, *24*, 77-91, 1997.

Percival, J.A., Archean Cratons, in *Searching for Diamonds in Canada*, edited by D.G. Richardson, R.N.W. DiLabio, and K.A.Richardson, *Open File Report 3228*, pp. 161-169, Geol. Surv. Can., 1996.

Pinet, C., and C. Jaupart, The vertical distribution of radiogenic heat production in the Precambrian crust of Norway and Sweden: Geothermal implications, *Geophys. Res. Lett.*, *14*, 260-263, 1987.

Pollack, H.N., and D.S. Chapman, On the regional variation of heat flow, geotherms and lithospheric thickness, *Tectonophys.*, *38*, 279-296, 1977.

Press, W.H., S.A. Flannery, S.A. Teukolsky, and W.T. Vetterling, *Numerical Recipes: The Art of Scientific Computing*, 818 pp. Cambridge Univ. Press, New York, 1986.

Ross, J.V., The nature and rheology of the Cordilleran upper mantle of British Columbia: Inferences from peridotite xenoliths, *Tectonophys.*, *100*, 321-357, 1983.

Rudnik, R.L., W.F. McDonough, and R.J. O'Connell, Thermal structure, thickness and composition of continental lithosphere, *Chem. Geol.*, *145*, 399-415, 1998.

Russell, J.K., Metamorphism of the Thompson Nickel Belt gneisses, Paint Lake, Manitoba, *Can. J. Earth Sci.*, *18*, 191-209, 1981.

Sass, J.H., and A.H. Lachenbruch, Thermal regime of the Australia continental crust, in *The Earth, Its Origin, Structure and Evolution*, edited by M.W. McElhinny, pp. 301-352, Academic Press, San Diego, Calif., 1979.

Sass, J.H., A.H. Lachenbruch, and A.M. Jessop, Uniform heat flow in a deep hole in the Canadian shield and its paleoclimatic implications, *J. Geophys. Res.*, *76*, 8586-8596, 1971.

Schatz, H.F., and G. Simmons, Thermal conductivity of Earth minerals at high temperatures. *J. Geophys. Res.*, *77*, 6966-6983, 1972.

Schulze, D.J., Kimberlites in the vicinity of Kirkland Lake and Lake Timiskaming, Ontario and Québec, in *Searching for Diamonds in Canada*, edited by A.N. LeCheminant, et al., *Open File Rep. 3228*, pp. 73-78, Geol. Surv. Can., 1996.

Sclater, J.G., C. Jaupart, and D. Galson, The heat flow through oceanic and continental crust and the heat loss of the Earth, *Rev. Geophys. 18*, 269-311, 1980.

Stacey, F.D., *Physics of the Earth*, 3rd ed., 462 pp., Brookfield, Brisbane, Australia, 1992.

Thompson, P.H., I. Russell, D. Paul, J.A. Kerswill, and E. Froese, Regional geology and mineral potential of the Winter Lake - Lac de Gras area (76D W1/2, 86A E1/2), central Slave Province, Northwest Territories, in *Current Research 1995-C*, pp. 107-119, Geol. Surv. Can., 1995a.

Thompson, P.H., A.S. Judge, and T.J. Lewis, Thermal properties of rock units in the Winter lake - Lac-de Gras area, central Slave province - Implications for diamond genesis, in *Current Research, 1995-E*, pp. 125-135, Geol. Surv. Can., 1995b.

Thompson, P.H., A.S. Judge, and T.J. Lewis, Thermal evolution of the lithosphere in the central Slave Province: Implications for diamond genesis, in *Searching for Diamonds in Canada*, edited by D.G. Richardson, R.N.W. DiLabio, and K.A. Richardson, *Open File Rep. 3228*, 151-160, Geol. Surv. Can., 1996.

Turcotte, D.L., and G. Schubert, *Geodynamics: Applications of Continuum Physics to Geological Problems*, 450 pp., John Wiley, New York, 1982.

M.G. Kopylova and J.K. Russell, Igneous Petrology Laboratory, Geological Sciences Division, Earth and Ocean Sciences, University of British Columbia, Vancouver, British Columbia, Canada V6T 1Z4. (Mkopylov@eos.ubc.ca; russell@perseus.geology.ubc.ca)

(Received March 2, 1998; revised December 29, 1998; accepted January 7, 1999.)